OPTIMIZING THE MICROSTRUCTURE OF LOW-REM ND-FE-B SINTERED MAGNET USING $Dy_3Co_{0.6}Cu_{0.4}H_x$ ADDITION

[1,2]Pavel A. PROKOFEV, [1]Natalia B. KOLCHUGINA, [1]Gennadiy S. BURKHANOV, [2]Alexander A. LUKIN, [1,3]Yurii S. KOSHKID'KO, [4]Katerina SKOTNICOVA, [4]Tomas CEGAN, [3]Henryk DRULIS, [3]Tatyana ROMANOVA, [1]Nikolay A. DORMIDONTOV

[1]Baikov Institute of Metallurgy and Materials Science, Russian Academy of Sciences, Moscow, Russian Federation, natalik014@yandex.ru, pav3387@yandex.ru

[2]JSC SPETSMAGNIT", Moscow, Russian Federation, lukinaalukin@rambler.ru

[3]Institute of Low Temperature and Structure Research, Polish Academy of Sciences, Wroclaw, Poland, EU HDrulis@int.pan.pl

[4]Vysoka Skola Banska - Technical University of Ostrava, Czech Republic, EU, Katerina.Skotnicova@vsb.cz

https://doi.org/10.37904/metal.2019.954

Abstract

In recent years, the application of various additions (hydrides, oxides, intermetallic compounds, etc.) to powder mixtures for manufacturing Nd-Fe-B magnets shows promise as the method that allows one to increase the hysteretic characteristics of the magnets at the expense of realized grain-boundary diffusion and grain-boundary structuring processes. The hysteretic characteristics of sintered Nd-Fe-B magnets are highly sensitive to their microstructure and composition of phases. This paper is focused on the coercivity enhancement of the near-stoichiometric $Nd_2Fe_{14}B$-based magnet by optimizing microstructure, which included processes of grain boundary diffusion and grain boundary structuring via the application of hydrogenated $Dy_3Co_{0.6}Cu_{0.4}H_x$ compound added to the powder mixture. The base alloy having the composition Nd-24.0, Pr-6.5, Dy-0.5, B-1.0, Al-0.2, Fe-balance was prepared by strip-casting technique and subjected to hydrogen decrepitation during heating to 270 °C in a hydrogen flow at a pressure of 0.1 MPa and subsequent 1 h holding at this temperature. $Dy_3Co_{0.6}Cu_{0.4}$ alloy was prepared by arc melting in an argon atmosphere and subjected to homogenizing annealing at 600 °C for 90 h. The subsequent hydrogenation under the conditions used for the decrepitation of the strip-cast alloy. The phase composition of $Dy_3Co_{0.6}Cu_{0.4}$ was studied by X-ray diffraction analysis, DTA and scanning electron microscopy, electron microprobe analysis. Additions of the hydrogenated compound to Nd-Fe-B-based sintered magnets allow us to manufacture magnets with Br = 1.34 T and jHc = 1120 kA/m. The microstructure, phase composition and distributions of REM, Co, Cu for the prepared magnets were investigated by SEM/EDX method. Stability of structure-sensitive parameter, namely, the coercive force jHc of the sintered magnet prepared with 2 wt% of $Dy_3Co_{0.6}Cu_{0.4}H_x$ addition was studied.

Keywords: Grain boundary diffusion, Nd-Fe-B magnets, hydrogenation, microstructure

1. INTRODUCTION

Currently, many attempts have been taken to reduce the heavy rare-earth consumption of high-coercivity Nd-Fe-B sintered magnets. Some progress has been achieved in using Dy and/or Tb in various forms, such as oxides, fluorides, hydrides, intermetallic compounds and alloys to realize approaches named grain boundary diffusion (GBD) [1-3] and grain boundary structuring (GBS) [4-8]. The application of binary mixtures with the aforementioned material allows one to improve the structure of boundary phases and grain boundaries of the main magnetic phase and to realize the diffusion of required component of alloy directly through boundaries. It has been demonstrated that through controlling the process time and temperature of GBD processes, the coercivity of the magnet can be greatly enhanced without sacrificing the remanence.

It was shown in our previous studies that Tb and Dy hydride additions allow us to increase both the coercive force along with a slight decrease in the remanence [9] and to increase the stability of properties of magnets during low-temperature annealing [10], respectively.

The grain boundary restructuring with rare-earth-rich low-melting compounds added to base low-alloyed Nd-Fe-B-based compositions in the course of technological processing was realized in [4] with $(Pr,Nd)_6Fe_{13}Cu$, [5] with $Dy_{32.5}Fe_{62}Cu_{5.5}$, [6] with $Dy_{69}Ni_{31}$, [11] with $Dy_{88}Mn_{12}$ (wt%) composition, [12] with $Pr_{34.4}Co_{65.6}$ (wt. %), and [13] with $Dy_{82.3}Co_{17.7}$ (wt%) that is the low-melting eutectic composition. It was shown that intrinsic coercivity increases obviously with the addition of $Dy_{82.3}Co_{17.7}$ and the maximum intrinsic coercivity is obtained when the content of $Dy_{82.3}Co_{17.7}$ was 2 wt%. At the same time, the remanence and maximum energy product decrease slightly with the increase of the $Dy_{82.3}Co_{17.7}$ content. By adding a small amount of $Dy_{82.3}Co_{17.7}$, the coercivity is improved greatly, and the irreversible loss is decreased sharply. The increase in the Curie temperature of the magnets suggests that Co atoms have entered into the 2:14:1 main phase. Microstructural analysis indicates that a well-developed core-shell structure was formed in the magnets with the addition of $Dy_{82.3}Co_{17.7}$. In all cases in using compositions with a heavy rare-earth metal, it was enriched in the outer region of the $Nd_2Fe_{14}B$ matrix grains during the sintering process, which favored to substitute for Nd in matrix grains to form the $(Nd,Dy)_2Fe_{14}B$ core-shell phase.

This paper is focused on optimizing the microstructure of the near-stoichiometric $Nd_2Fe_{14}B$-based magnet, which included the grain boundary diffusion and grain boundary structuring processes via the application of hydrogenated $Dy_3Co_{0.6}Cu_{0.4}H_x$ composition added to powder mixture.

2. EXPERIMENTAL

The $Dy_3(Co_{1-x}Cu_x)$ alloy with x = 0.4 was prepared by arc melting of starting components (distilled Dy-99.9 at%, electrolytic Co (K-1 grade), and oxygen-free copper) in an argon atmosphere using a water-cold copper bottom and a nonconsumable tungsten electrode. The ingot was subjected to homogenizing annealing at 600°C for 90 h. The ingot was subjected to hydrogenation in two regimes; (regime 1) conditions applied for the strip-casting alloy, namely, the heating to 270 °C in a hydrogen flow at a pressure of 0.1 MPa and subsequent 1 h holding at this temperature, and (regime 2) heating in hydrogen atmosphere and holding at 700 °C in a glass Sieverts-type apparatus were used. In the case of heating up 700 °C, the hydrogenation up to the $Dy_3Co_{0.6}Cu_{0.4}H_x$ composition with x = 8.26 was realized. We assume that such hydrogen content corresponds to the complete hydrogenation of dysprosium to a dysprosium hydride.

The phase composition of the $Dy_3Co_{0.6}Cu_{0.4}$ and $Dy3Co0.6Cu_{0.4}H_x$ compositions with x = 8.26 was studied by X-ray diffraction (XRD) analysis using an Ultima IV (Rigaku», Japan) diffractometer equipped with a "D/teX" detector, CuKα radiation; the scanning step is 0.001°. X-ray diffraction patterns were process and the phase composition of the alloy was determined using PowderCell software. The data on the crystal structure type, lattice parameters, and crystallographic positions of atoms in the Dy-Co, Dy-Cu, and H-Dy system alloys were used to simulate theoretical XRD patterns [14-16]. The differential thermal analysis of the hydrogenated and dehydrogenated $Dy_3Co_{0.6}Cu_{0.4}H_x$ composition was carried out in an argon atmosphere at a heating / cooling rate of 30 °C/min using a Setaram Setsys -1750 installation.

The mixture of the $Dy_3Co_{0.6}Cu_{0.4}$ alloy and hydrogen-decrepitated strip-casting alloy (hydrogenated at 270 °C for 1h) was subjected to fine milling for 40 min to an average particle size of 3 μm using a vibratory mill and isopropyl alcohol medium. After wet compaction of the pulp in a transverse magnetic field of 1500 kA/m, blanks of magnets were sintered at T = 1080 °C for 2 h and subjected to optimum heat treatment at 500 °C for 2 h. The high-resolution field emission gun-scanning electron microscope QUANTA 450 FEG equipped with an EDX APOLLO X microprobe was used for the investigation of microstructure and chemical composition of magnet sample. The subsequent temperature stepped heat treatments in a temperature range of 400 - 900 °C were used. The hysteretic properties were measured using a hysteresisgraph.

3. RESULTS AND DISCUSSION

3.1. X-ray diffraction analysis

Figure 1 shows X-ray diffraction pattern of the $Dy_3Co_{0.6}Cu_{0.4}$ alloy subjected to prolonged annealing in an argon atmosphere. Unmarked reflections (**Figure 1**) belong to the main $Dy_3(Co,Cu)$ phase; marked reflections correspond to Dy(Cu,Co) phase based on DyCu [14,15]. The analysis of crystal structures of the found compounds and construction of theoretical XRD patterns for the simulated structures allowed us to determine variations of lattice parameters of phases alloyed with Co for $Dy(Cu_{1-y}Co_y)$ and with Cu for $Dy_3(Co_{1-x}Cu_x)$ (see **Table 1**).

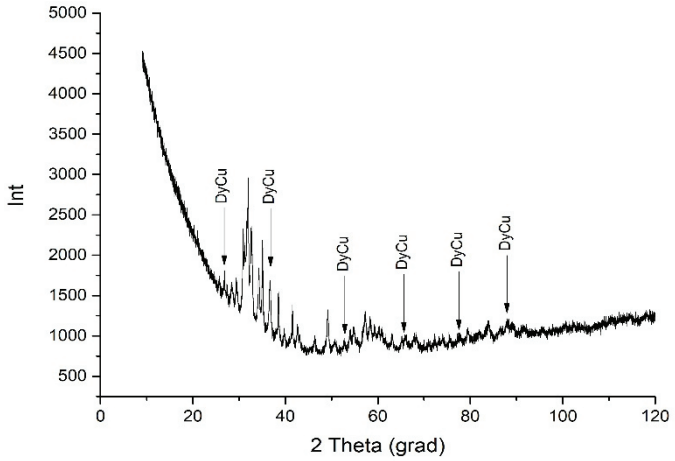

Figure 1 X-ray diffraction pattern of the $Dy_3(Co,Cu)$ alloy

Table 1 Crystallographic parameters of the phases in the $Dy_3(Co,Cu)$ alloy

№	Compound	Space group	C	*a* (nm)	*b* (nm)	*c* (nm)	References
1	Dy_3Co	Pnma	Fe_3C	0.6965	0.9341	0.6233	[14]
2	$Dy_3(Co_{1-x}Cu_x)$	Pnma	Fe_3C	0.69331	0.93847	6.2564	This work
5	DyCu	$Pm\bar{3}m$	CsCl	0.3461	0.3461	0.3461	[15]
6	$Dy(Cu_{1-y}Co_y)$	$Pm\bar{3}m$	CsCl	0.34522	0.34522	0.34522	This work

As is seen, the alloying of the binary compounds with Co and Cu does not change the crystal structure type of the binary compounds. The phases present in the alloy are alloyed modifications of the binary compounds in accordance with their phase diagrams [14,15].

As is seen, the substitution of Cu for Co changes the lattice parameters: the lattice parameters *b* and *c* increase because the radius of Cu atoms (0.128 nm) is higher than that of Co atoms (0.125 nm). However, the decrease of the lattice parameter *a* takes place. This is likely to be due to the fact that copper atoms substitute for cobalt atoms only in certain positions. Similarly to [17,18], the presence of a compound based on $Dy_{12}Co_7$ is possible.

We assume that the solidification of the alloy occurs via the primary formation of Dy_3Co-based phase by peritectic reaction; the DyCu-based compound is the secondary phase. According to the Co-Dy phase diagram, the solidification path may include the formation of the $Dy_{12}Co_7$-based compound by peritectic reaction.

3.2. Interaction of $Dy_3(Co,Cu)$ alloy with hydrogen

Saturation of the alloy $Dy_3Co_{0.6}Cu_{0.4}$ with hydrogen led to the embrittlement of the alloy, i.e., to obtaining the powder material suitable for the further introduction of the composition into the Nd-Fe-B magnetic alloy powder

during cooperative milling. **Figure 2(a)** shows X-ray diffraction analysis of the alloy $Dy_3Co_{0.6}Cu_{0.4}$ subjected to hydrogenation.

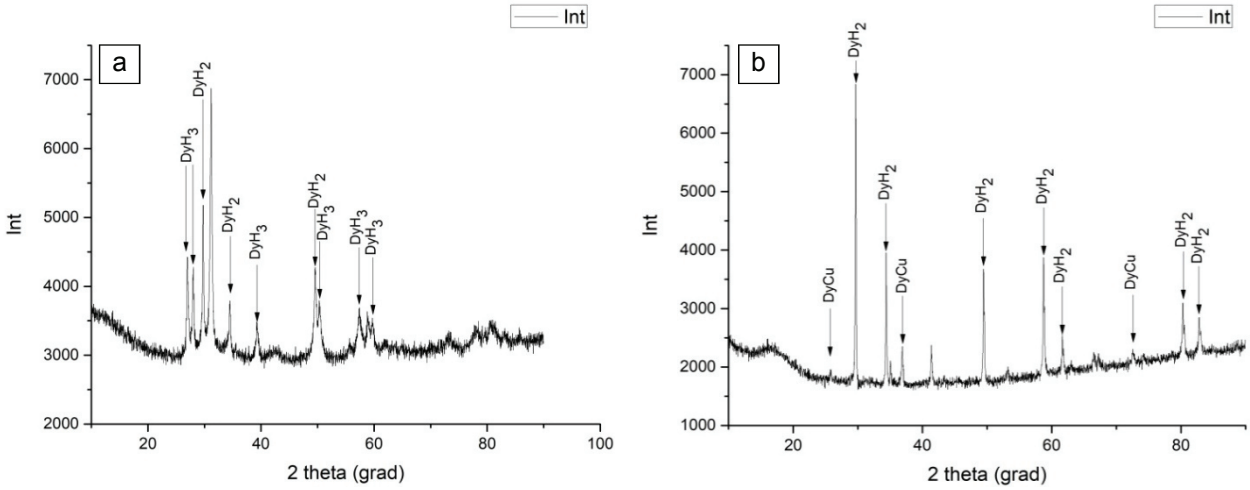

Figure 2 X-ray diffraction pattern of the $Dy_3(Co,Cu)$ alloy after saturation with hydrogen (a) and after thermal desaturation process (DTA) (b)

The hydrogenated composition contains DyH_2 [19] and DyH_3 [20]. Unmarked reflections in **Figure 2(a)** correspond to $Dy_3(Co,Cu)$ phase. Small quantities of $Dy_3(Co,Cu)$ and Dy(Cu,Co) phases didn't interact with hydrogen. Also, is possible the presence of a thin mechanical mixture of Cu and Co.

Figure 2(b) shows X-ray diffraction analysis of the alloy $Dy_3Co_{0.6}Cu_{0.4}$ H_x subjected to thermal dehydrogenation (upon heating during DTA). Sample was heated up to 700 °C (**Figure 3**). After heating, we observed presence of DyH_2 and small quantities of $Dy_3(Co,Cu)$ and Dy(Cu,Co) phases; DyH_3 is absent. Also, the presence of a thin mechanical mixture of Cu and Co is possible.

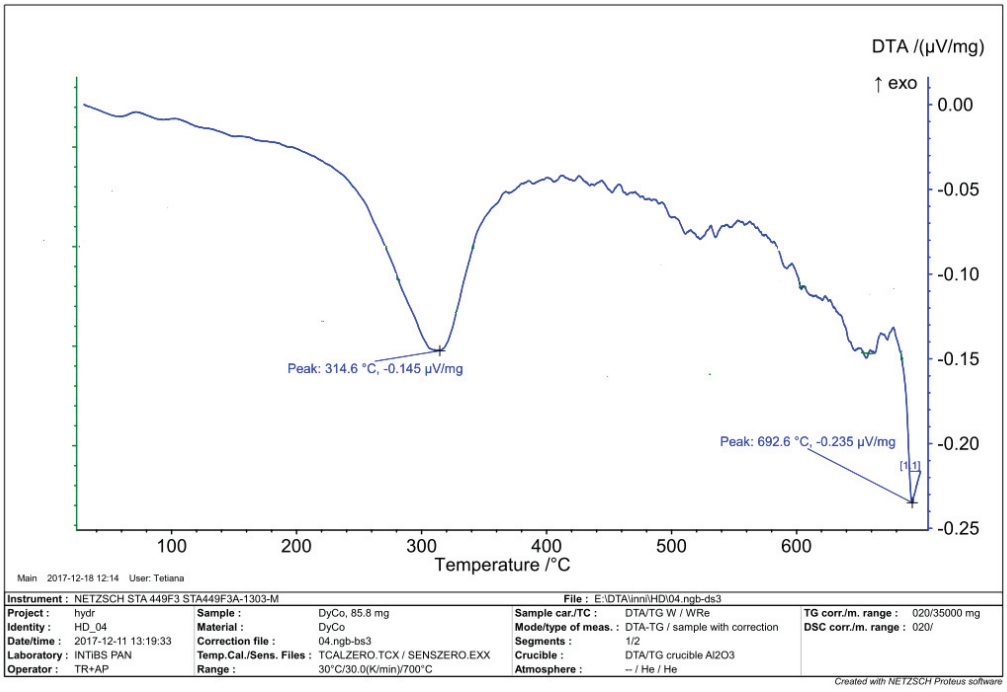

Figure 3 DTA curve of $Dy_3(Co,Cu)H_{8.26}$ sample

According to the DTA data (**Figure 3**), the decomposition of DyH_3 begins at temperature ~314 °C, which confirmed by literature data [16]. Between ~314 °C and ~690 °C there aren't any reactions. At temperature above ~ 690 ° C, in accordance with the Dy-H [16] diagram, the solid solution of hydrogen in dysprosium decomposes to form dysprosium. However, the thermal effects at temperatures above 600 °C can correspond to melting of one the metallic components of the alloy, nevertheless accompanying to the significant weight loss.

The formation of Dy-hydride indicates the possibility of the composition to be used as additions in manufacturing sintered Nd-Fe-B magnets.

3.3. Microstructure and electron microprobe analysis of sintered NdFeB-based magnet

In accordance with the microprobe analysis data showed in **Table 2**, the microstructure (**Figure 4**) is characterized by the presence of four structural components with different chemical composition (structural components were marked).

Table 2 Chemical analysis of Nd-Fe-B sintered magnet prepared from the powder mixture with 2 wt% of $Dy_3Co_{0.6}Cu_{0.4}H_x$ compound (in at%)

Element/phase	O_K	Dy_M	Al_K	Nb_L	Pr_L	Nd_L	Fe_K	Co_K	Cu_K
Phase_1	6.6	0.9	0.5	0.2	2.9	9.7	77.6	1.1	0.5
Phase_2_1	15.7	1.1	0.5	0.3	8.9	25.6	32.7	1.1	14.1
Phase_2_2	6.0	6.1	0.0	1.2	11.2	29.4	44.1	1.1	1.0
Phase_2_3	8.2	0.8	1.4	0.1	11.3	22.8	47.1	2.7	5.6
Phase_2_4	6.8	2.9	0.9	0.2	17.8	40.6	21.1	3.7	6.1
Phase_3_1	47.7	0.9	0.2	0.2	7.4	22.3	20.2	0.5	0.6
Phase_3_2	67.0	1.3	0.0	0.1	7.2	20.9	2.9	0.3	0.4
Phase_3_3	64.9	1.4	0.0	0.2	7.7	21.8	3.7	0.3	0.2
Phase_4_1	14.7	0.4	0.1	40.7	0.5	1.5	41.7	0.3	0.2

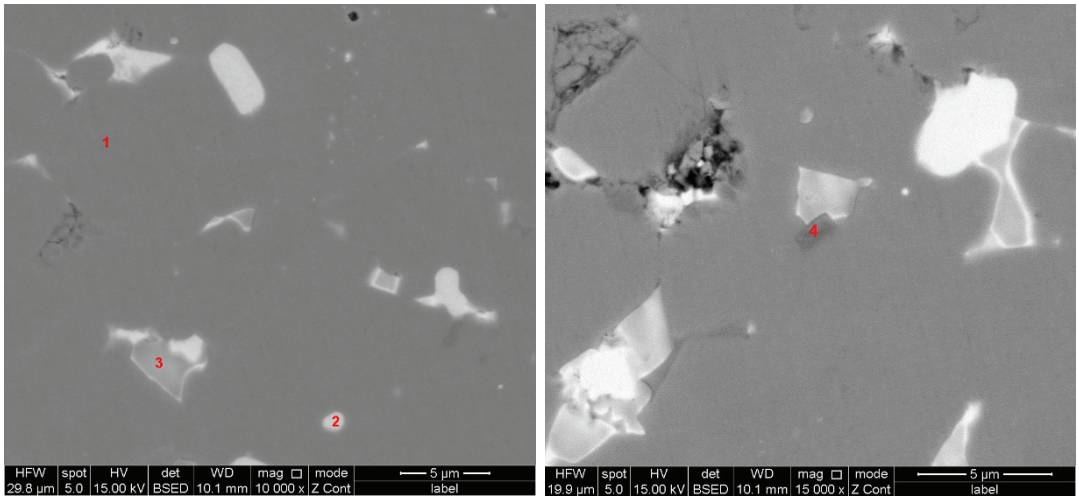

Figure 4 The microstructure of Nd-Fe-B sintered magnet prepared from the powder mixture with 2 wt% $Dy_3Co_{0.6}Cu_{0.4}H_x$; (marked phases correspond to those in **Table 2**)

The chemical composition of phase 1 (the average values from three analysis) is close to the stoichiometry of $(Nd,R)_2Fe_{14}B$. The presence of Dy in the matrix alloy doesn't allow us to conclude that the core-shell structure

was formed, but the presence of cobalt in 2:14:1 grains demonstrates the possibility of micro-alloying through the use of hydrogenated low-melting compounds (lower then the sintering temperature of Nd-Fe-B magnets). The Nd-rich phase (phase 2) is characterized by variable composition. In accordance with the microprobe analysis data, there is a strong difference in the content of Dy and Cu in the Nd-rich phases. This may indirectly indicate the partial occurrence of the grain boundary diffusion process. Phase 3 (**Figure 4**) corresponds to oxide phases. In accordance with the literature data [21-22], phase 3 is an oxide phase based on: NdO, Nd_2O_3, NdO_2. The presence of a phase based on Fe-Nb in triple junctions was observed (phase 4, **Figure 4**). This fact may be related to impurities in matrix alloy.

3.4. Dependence of the coercive force on temperature ($_jH_c$)

The magnetic properties ($_jH_c$) of the magnets (see **Table 3**) prepared with the hydrogenated $Dy_3Co_{0.6}Cu_{0.4}$ alloy are lower than those in the case of DyH_2 [23]. One of the causes is incomplete hydrogenation of alloy and incomplete occurrence of grain boundary diffusion of Dy. This fact was confirmed by X-ray diffraction. The small quantity of $Dy_3(Co,Cu)$ phase is present in the $Dy_3Co_{0.6}Cu_{0.4}$ sample after hydrogenation. However, the value of B_r in case of $Dy_3Co_{0.6}Cu_{0.4}H_x$ is higher than that in the case of DyH_2, it may be due to difference in the Dy content in chemical composition of 2:14:1 phase. The difference in REM and Cu contents in the Nd-rich phases provides to lower value of H_k in case of Nd-Fe-B-based magnets with 2 wt% $Dy_3Co_{0.6}Cu_{0.4}H_x$.

Table 3 Magnetic properties of sintered magnets prepared with 2 wt% $Dy_3Co_{0.6}Cu_{0.4}H_x$ (with x = ~2) and subjected to optimum heat treatment at 500 °C for 2 h

Addition / Annealing conditions	B_r (T)	$_jH_c$ (kA/m)	H_k (kA/m)	BH_{max} (kJ/m^3)
$Dy_3Co_{0.6}Cu_{0.4}H_x$ \ optimum	1.34	1120	968	336
DyH_2 / optimum	1.29	1309	1262	322

Figure 5 shows variations of the coercive force ($_jH_c$) with changing heat treatment (HT) temperature. As seen from the curve, the value of $_jH_c$ after HT in a range of temperatures 475-500 °C rapidly increases.

We assume the optimum HT for this type of magnets is in the range of 475 to 500 °C like in case of magnets considered in [17]. Subsequent HT in this temperature range will lead to increase in the coercive force for magnets with 2 wt% $Dy_3Co_{0.6}Cu_{0.4}H_x$ after optimum heat treatment (500 °C).

4. CONCLUSIONS

The phase composition of the $Dy_3Co_{0.6}Cu_{0.4}$ alloy in the initial homogenized and hydrogenated states was studied. The alloy in the homogenized state contained $Dy_3(Co,Cu)$ and Dy(Cu,Co) phases. During hydrogenation of the two-phase alloy, the disproportionation or hydrogenolysis process took place, which, whatever the two-phase composition of initial alloy, resulted in the formation of DyH_{2-3} hydride and probably fine (Co+Cu) mixture with small quantities of $Dy_3(Co,Cu)$ and Dy(Cu,Co). The possibility for using $Dy_3Co_{0.6}Cu_{0.}4H_x$ addition to the powder mixture for manufacturing of sintered permanent magnet was shown.

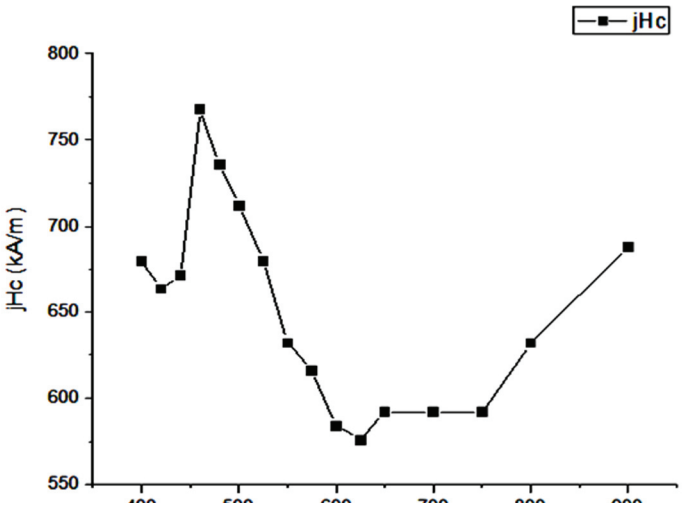

Figure 5 The temperature dependence of the $_jH_c$ of Nd-Fe-B-based magnet with 2 wt% of $Dy_3Co_{0.6,}Cu_{0.4}$

ACKNOWLEDGEMENTS

This study was supported by the Ministry of Education and Science of the Russian Federation, agreement no. 14.616.21.0093 (unique identification number RFMEFI61618X0093) and the Ministry of Education, Youth, and Sports of the Czech Republic, project no. LTARF18031.

REFERENCES

[1] LIU, W. Q., SUN, H., YI, X. F., LIU, X. C., ZHANG, D. T., YUE, M. and ZHANG, J. X. Coercivity enhancement in Nd-Fe-B sintered permanent magnet by Dy nanoparticles doping. *Journal of Alloys and Compounds.*, 2010. vol. 501, pp. 67-69.

[2] SEPEHRI-AMIN, H., LIU, L., OHKUBO, T., YANO, M., SHOJI, T., KATO, A., SCHREFL,T. and HONO, K. Microstructure and temperature dependent of coercivity of hot-deformed Nd-Fe-B magnets diffusion processed with Pr-Cu alloy. *Acta Materialia.* 2015. vol. 99, pp. 297-306.

[3] KOMURO, M., SATSU, Y. and SUZUKI, H. Increase of coercivity and composition distribution in fluoride-diffused NdFeB sintered magnets treated by fluoride solutions. *IEEE Transactions of Magnets.* 2010. vol. 46, pp. 3831-3833.

[4] NI, J., MA, T. and YAN, M. Improvement of corrosion resistance in Nd-Fe-B magnets through grain boundaries restructuring. *Materials Letters.* 2012. vol. 75, pp. 1-3.

[5] LIANG, L., MAN, T., ZHANG, P., JIN, J. and YAN, M. Coercivity enhancement of NdFeB sintered magnets by low melting point $Dy_{32.5}Fe_{62}Cu_{5.5}$ alloy modification. *Journal of Magnetism and Magnetic Materials.* 2014, vol. 355, pp. 131-135.

[6] LIU, X., WANG, X., LIANG, L., ZHANG, P., JIN, J., ZHANG, J., MAN, T. and ANN, M. Rapid coercivity increment of Nd-Fe-B sintered magnets by $Dy_{69}Ni_{31}$ grain boundary restructuring, *Journal of Magnetism and Magnetic Materials.* 2014. vol. 370, pp. 76-80.

[7] GUO, S., CHEN, R. J., DING, Y., YAN, G. H., LEE, D. and YAN, A. R. Effect of DyH_x addition on the magnetic properties and microstructure of $Nd_{14.1}Co_{1.34}Cu_{0.04}Fe_{bal.}B_{5.84}$ magnets. *Journal of Physics: Conference Series.* 2011. vol. 266, pp. 16-19.

[8] KIM, T.-H., LEE, S.-R., KIM, H.-J., LEE, M.-W. and JANG, T.-S. Magnetic and microstructural modification of the Nd-Fe-B sintered magnet by mixed DyF_3/DyH_x powder doping. *Journal of Applied Physics.* 2014. vol. 115, no. 17, pp. 17A763.

[9] LUKIN, A., KOLCHUGINA, N. B., BURKHANOV, G. S., KLYUEVA, N. E. and SKOTNICOVA, K. Role of terbium hydride additions in the formation of microstructure and magnetic properties of sintered Nd-Pr-Dy-Fe-B magnets. *Inorganic Materials. Applied Research.* 2013. vol. 4, pp. 256-259.

[10] BURKHANOV, G. S., LUKIN, A. A., KOLCHUGINA, N. B., KOSHKID'KO, Yu. S., DORMIDONTOV, A. G., SKOTNICOVÁ, K., ZIVOTSKY, O., ČEGAN, T. and SITNOV, V. V. Effect of low-temperature annealing on the structure and hysteretic properties of Nd-Fe-B magnets prepared with hydride-containing mixtures. In *REPM 2014: 23rd International Workshop on Rare-Earth and Future Permanent Magnets and Their Applications*. Annapolis, USA, 2014. pp. 367-369.

[11] Li, X., LIU, S., CAO, X., ZHOU, B., CHEN, L., YAN, A. and YAN, G. Coercivity and thermal stability improvement in sintered Nd-Fe-B permanent magnets by intergranular addition of Dy-Mn alloy. *Journal of Magnetism and Magnetic Materials.* 2016. vol. 407, pp. 247-251.

[12] JIN, C., CHEN, R., YIN, W., TANG, X., WANG, Z., JU, J., LEE, D. and YAN, A. Magnetic properties and phase evolution of Nd-Fe-B magnets with intergranular addition of Pr-Co alloy. *Journal of Alloys and Compounds.* 2016. vol. 670. pp. 72-77.

[13] ZHANG, X., GUO, S., YAN, C-J., CAI, L., CHEN, R., LEE, D. and YAN, R. Improvement of the thermal stability of sintered Nd-Fe-B magnets by intergranular addition of $Dy_{82.3}Co_{17.7}$. *Journal of Applied Physics.* 2014, vol. 115, pp. 17A757.

[14] *Binary Alloy Phase Diagram*. Ed. by T.B. Massalski, H. Okamoto, P.R. Subramanian, L. Kacprzak, 2nd ed. Materials Park, Ohio: ASM International. 1990. 3589 p.

[15] MASSALSKI, T.B., OKAMOTO, H., SUBRAMANIAN, P.R., KACPRZAK, L., eds. *Binary Alloy Phase Diagrams*, Ohio: International Metallographic Society. 1990. 3 589 p.

[16] PREDEL, B. *Phase Equilibria, Crystallographic and Thermodynamic Data of Binary Alloys' of Landolt-Börnstein - Group IV. Physical Chemistry.* 1st ed. Berlin: Springer-Verlag 1995. 337 p.

[17] BURKHANOV, G. S., KOLCHUGINA, N. B., KOSHKID`KO, Y. S., CWIK, J., SKOTNICOVA, K., CEGAN, T., PROKOF`EV, P. A., DRULIS, H. and HACKEMER, A. Structure and phase composition of $Tb_3Co_{0.6}Cu_{0.4}$ alloys for efficient additions to Nd-Fe-B sintered magnets. In *METAL 2017 - 26th International Conference on Metallurgy and Materials*, Conference Proceedings. 2017, Pages 1775-1781.

[18] PROKOF'EV P. A., KOLCHUGINA N. B., BURKHANOV G. S., LUKIN A. A., KOSHKID'KO Y. S., SKOTNICOVA K., CEGAN T., ZIVOTSKY O. and KURSA M. Phase formation in the Tb-Co-Cu system in a range of Tb_3(Co,Cu) compound. In *METAL 2018: 27th International Conference on Metallurgy and Materials*. Ostrava: TANGER. 2018. pp. 1685-1692.

[19] The Materials Project. 2019. [viewed 2019-04-20]. Available from: https://materialsproject.org/materials/mp-1191571/.

[20] The Materials Project. 2019. [viewed 2019-04-20]. Available from: URL: https://materialsproject.org/materials/mp-24151

[21] KIM, T-H., LEE, S-R., NAMKUMG, S. et al. A study on the Nd-rich phase evolution in the Nd-Fe-B sintered magnet and its mechanism during post-sintering annealing. *Journal of Alloys and Compounds.* 2012. vol. 537, pp. 261-268.

[22] WANG, S.C. and LI, Y. In situ TEM study of Nd-rich phase in NdFeB magnet. *Journal of Magnetism and Magnetic Materials.* 2005. vol. 285, pp. 177-182.

[23] BURKHANOV G. S., KOLCHUGINA N. B., LUKIN A. A., KOSHKID`KO Y. S., CWIK J., SKOTNICOVA K. and SITNOV V. V., Structure and Magnetic Properties of Nd-Fe-B Magnets Prepared from DyH_2-Containing Powder Mixtures. *Inorganic Materials: Applied Research.* 2018. vol. 9, pp. 509-516.